Directional Force Sensation by Asymmetric Oscillation From a Double-Layer Slider-Crank Mechanism

Tomohiro Amemiya[1]
Researcher
NTT Communication Science Laboratories,
Nippon Telegraph and Telephone Corporation,
3-1 Morinosato Wakamiya,
Atsugi, Kanagawa,
243-0198 Japan
e-mail: t-amemiya@avg.brl.ntt.co.jp

Taro Maeda
Professor
Graduate School of Information Science and Technology,
Osaka University

By subjecting a small object in a handheld device to periodic translational motion with asymmetric acceleration (accelerated more rapidly in one direction than in the other), the holder typically experiences the kinesthetic illusion of being pushed or pulled continuously by the held device. We have been investigating the effect because of its potential application to a handheld, nongrounded, haptic device that can convey a sense of a continuous translational force in one direction. A one-degree-of-freedom haptic device based on a double-layer slider-crank mechanism was constructed based on the results of our previous research. Our results with the new haptic device show that (i) humans perceive directed force sensation by asymmetric oscillation, (ii) 5 counts/s is the best frequency to generate the force sensation, (iii) the ratio of the gross weight of the device and the weight of the reciprocating mass should be at least 16% for effective force perception, and (iv) the force perception is the same with the device held in either hand. [DOI: 10.1115/1.3072900]

Keywords: haptic display, perception, wearable and mobile computing, interaction, interface using sensory illusion

1 Introduction

Haptic feedback provides many potential benefits for the use of small portable handheld devices, and much research has pointed out some of these benefits for mobile devices (e.g., Refs. [1,2]). Vibration motors are common in cellular phones and gaming technologies and have been employed in research work such as the haptic kymograph of Kim et al. [3] and the handheld haptics of Maclean et al. [4]. However, in mobile devices, the haptic stimuli are limited to cutaneous ones, which are largely known as tactile ones, such as vibration generated from vibrators. This is because mobile devices have difficulty producing a kinesthetic sensation, not to mention that applying low-frequency forces to a user requires a fixed mechanical ground, which mobile haptic devices lack. To make force-feedback devices available outside the laboratory, ungrounded devices have been developed since ungrounded haptic feedback devices are more mobile and can operate over larger workspaces compared with grounded devices [5]. The performance of ungrounded haptic feedback devices has been shown to be less accurate than that of grounded ones in contact tasks. However, ungrounded haptic feedback devices can give results comparable to those that grounded ones do in boundary detection tests [6]. Unfortunately, typical ungrounded devices based on the gyroeffect (e.g., Ref. [7]) or angular momentum change (e.g., Ref. [8]) are unable to generate both constant and directional forces; they can generate only a transient rotational force (torque) sensation. In addition, Kunzler and Runde [9] pointed out that gyromoment displays are proportional to the mass, diameter, and angular velocity of the flywheel.

There are methods for generating sustained translational force without grounding, such as propulsive force or electromagnetic force. Recently, some ideas for generating both constant and directional forces without an external fulcrum have been proposed, such as using two oblique motors whose velocity and phase are controlled [10] and simulating kinesthetic inertia by shifting the center-of-mass of a device dynamically when the device is held with both hands [11].

The authors proposed a force perception method that can generate a sustained directional force sensation with no external grounding and designed and developed prototypes that generate the asymmetric back-and-forth motion of a small, constrained mass with a slider-crank mechanism [12,13] or spring-cam mechanism [14]. The method exploits the characteristics of human perception to generate a force sensation, using different acceleration patterns for the two directions to create a perceived force imbalance and thereby produce the sensation of directional pushing or pulling. Concretely, a strong acceleration is generated for a very brief time in the desired direction, while a weaker acceleration is generated over a longer period of time in the reverse direction. The weaker acceleration is not detected by the internal human haptic sensors, so the original position of the mass is "washed out." The result is that the user is tricked into perceiving a unidirectional force. This force can be made continuous by repeating the motions.

Our previous research has revealed the perceptual characteristics of the force sensation created by asymmetric acceleration [12–14]. This paper describes the development of a new prototype that, on the basis of our previous findings [12], was specially designed for use in the range 5–10 counts/s. We conducted three experiments to evaluate the new prototype and determine the criteria for designing the force displays. In experiment 1, we compared the perceptual effect of the different acceleration profiles, asymmetric and symmetric oscillations, with double-layer slider-crank mechanisms. In experiment 2, we determined the threshold of the ratio of the gross weight of the device and the weight of the reciprocating mass to perceive force sensation. In experiment 3,

[1]Corresponding author.

Contributed by the Engineering Simulation and Visualization Committee of ASME for publication in the JOURNAL OF COMPUTING AND INFORMATION SCIENCE IN ENGINEERING. Manuscript received August 31, 2007; final manuscript received July 15, 2008; published online February 9, 2009. Guest Editors: J. Oliver, M. Omalley, and K. Kesavadas.

we examined whether there is any difference in force perception when the new prototype is held with the dominant or nondominant hand.

2 System Description and Design

In the earlier prototype [12], circular motion at constant speed is transformed into a curvilinear motion by a swinging-block slider-crank mechanism. By physically connecting the end point of the curvilinearly moving linkage with a point on another slider that slides along a straight line, a reciprocating motion with asymmetric acceleration is generated. In addition, an antiphase tandem pair of identical mechanisms physically counteracts the swinging force generated by the motion of the linkages. In designing the new prototype, we examined several aspects of the old one to see where it could be improved or modified.

2.1 Size and Weight. The earlier prototype [12], which employed a swinging slider-crank mechanism, is 130 mm wide $\times$200 mm deep$\times$48 mm high and its gross weight is approximately 500 g.

Such a big and heavy device is unsuitable for integration into mobile devices. Heavy devices may also make force perception difficult because of the assumption of a constant Weber fraction. To perceive the force sensation effectively, it would be better to increase the weight of the reciprocating mass or to decrease the gross weight of the device. We adopted the latter solution for effective force perception (since the gross weight must be low for mobile devices).

Since linkages in the mechanism generate a side-to-side force, two horizontally aligned identical mechanisms were employed in the earlier prototype to cancel it. Slider-crank mechanisms must be wide enough for the linkages to move. It is therefore difficult to reduce the width of the plane on which they move. Instead, we designed two identical vertically aligned mechanisms to reduce the size of the device.

2.2 Reduction Gear Versus Direct Drive. The motor was one of the most important considerations in the design of the new prototype. Generally, the power of a motor is determined by its size. Since the motor in the new prototype would basically do no work (i.e., no energy is transferred), we desired a motor that can generate adequately large torque even if its power is low.

The reduction gear mechanism has been used in many motors to obtain a large torque, but there is a trade-off between rotational velocity and torque. In the new prototype, since the output frequency of the slider is at most 20 Hz (1200 rpm for the crank), the rotational velocity of motor with the reduction gear mechanism is large enough for the new prototype. In contrast, a direct drive mechanism (i.e., no reduction gear mechanism) is advantageous for reducing noise. However, its performance depends on the motor's specifications; a special motor would be required for the direct drive mechanism, and this would be impractical. By taking all of these things into account, we decided to adopt a small and light motor with the reduction gear mechanism.

In addition, the flywheel effect of the motor is the second power of the reduction ratio in the reduction gear mechanism. If no servo control is used, the torque change is dependent on flywheel characteristics. Therefore, if the flywheel effect is large enough, constant speed control will be possible by using a simple open-loop control, such as an electric governor function.

The most efficient rpm range of small motors is approximately 5000–10,000. Therefore, a 1/10 reduction rate of the gears would be appropriate for utilizing the most efficient rpm range, since output frequencies of under 10 counts/s are desired for well-perceiving force sensation.

2.3 Mechanism. The swing slider-crank mechanism is one way to generate asymmetric oscillation. There are other mechanisms for generating asymmetric oscillation, such as the spring-cam mechanisms [14], which would be beneficial from the standpoint of miniaturization. Regardless of the mechanism used, it is important that we understand the parameters of asymmetric oscillation and the effects of the gross weight of the device in designing ungrounded force displays. In addition, the swing slider-crank mechanism makes it easy to calculate the output acceleration from input speed as shown in the equations below, and it is therefore convenient for an experimental setup. Therefore, we adopted the swing slider-crank mechanism and do not discuss the other possible mechanisms further.

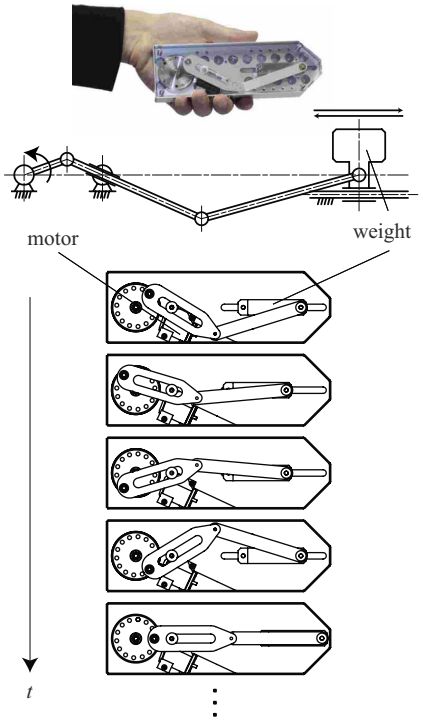

Fig. 1 Photograph and mechanism of the force display. The slider-crank mechanism outputs translational motion with asymmetric acceleration from a single-speed rotation input.

2.4 Implementation. The new prototype is based on a similar swinging slider-crank mechanism with a reduction gear mechanism (Fig. 1). It has two layers that work to cancel the effect of the side-to-side force produced by the linkages. The size is decreased by 21% compared with the earlier one ($56\times175\times27$ mm^3). The weight is decreased by 50% (to 250 g), although the weight of the reciprocating mass is the same (40 g). The device uses a small dc motor (1724T006SR; Faulhaber, 2.58 W, 27 g). The motor pinion engages two crown gears that face each other. The crown gears work as cranks in the mechanism. The structure is shown in Fig. 2. The motor in the new prototype is controlled to rotate at a constant speed by a motor amplifier with an electronic governor function: The motor is controlled by current control. The device converts the single-speed rotational cyclic movement of the motor into asymmetric translational cyclic movement with asymmetric acceleration via the gears and the swinging slider-crank mechanism.

3 Experiment 1: Comparison Between Different Acceleration Profiles

We determined the percent-correct scores (i.e., how often the perceived force direction matched the x-direction) at several motor rotational frequencies using two stimuli with different acceleration profiles. The participants made a binary judgment of the perceived force direction (forward or backward, as defined in Fig. 3).

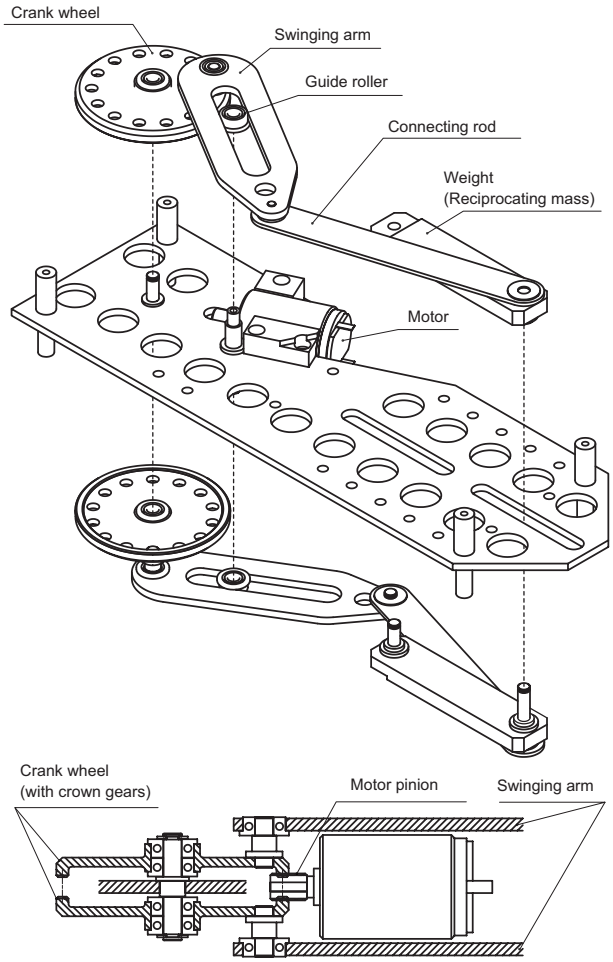

Fig. 2 Structure of the new force display. The force display has a double-layer arrangement that cancels the side-to-side force generated by linkage motion. The motor pinion engages two opposing crown gears. The crown gears work as cranks in the mechanism.

3.1 Method

3.1.1 Participants. Six normal healthy adults (five women and one man) aged between 24 and 33 years participated in this experiment. They had no known abnormalities of their tactile or kinesthetic sensory systems. All of them reported that they were right-handed. None were involved in the research project. All experiments in this research were approved by the Local Ethics Committee.

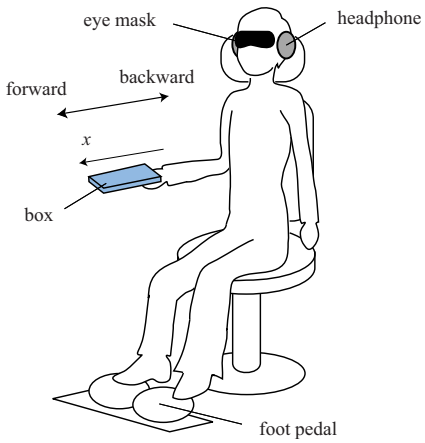

Fig. 3 Illustration of the body posture in experiment 1. The direction from the elbow to the wrist is forward, and the opposite is backward.

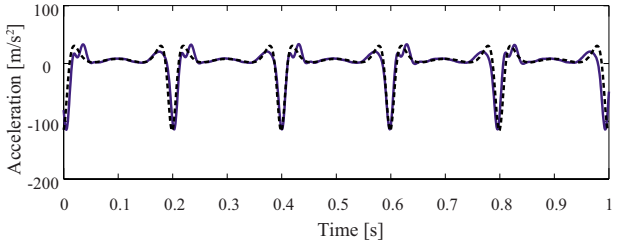

Fig. 4 Actual acceleration value of the apparatus for the test experiment (solid line) versus the calculated value (dotted line)

3.1.2 Stimuli and Apparatus. Two kinds of stimuli were used, test stimuli and control stimuli. Test stimuli were generated by asymmetric oscillation of a mass (hereafter called asymmetric acceleration). The actual and calculated acceleration values are shown in Fig. 4. Control stimuli were generated by symmetric oscillation of a mass (hereafter called symmetric acceleration). The actual and calculated acceleration values are shown in Fig. 5. Actual acceleration values were calculated by the position data of the weight, which were acquired with a laser sensor (Keyence Inc., LK-G150, 20 kHz sampling).

The mechanism generating each stimulus was covered with an aluminum box (56 mm wide × 175 mm deep × 27 mm high, ASUS 100) to prevent subjects discriminating the orientation from the shape and surface. The weight of the reciprocating mass was 40 g. The gross weight of the box was 250 g. The stroke of the reciprocating mass and the weight of linkages were adjusted to be identical. Each device had a mirror-symmetry pair of mechanisms that counteracted the effects of the motion of linkages, i.e., torque along the z-axis, on test stimuli (Figs. 6 and 7) and control stimuli (Figs. 8 and 9).

The motion of the weight in the swinging slider-crank mechanism is given by

$$x = r\cos\omega t + \mu(d - r\cos\omega t) + \sqrt{l_2^2 - \{r(\mu - 1)\sin\omega t\}^2} \quad (1)$$

where

$$\mu = \frac{l_1}{\sqrt{r^2 + d^2 - 2rd\cos\omega t}} \quad (2)$$

and $x=OD$, $r=OB$, $d=OA$, $l_1=BC$, $l_2=CD$, and $\omega t=AOB$ in Fig. 7. The t is time and ω is angular velocity. In the prototype, $r=15$ mm, $d=28$ mm, $l_1=60$ mm, and $l_2=70$ mm. Acceleration of test stimuli is given by the second derivative with respect to time of x as

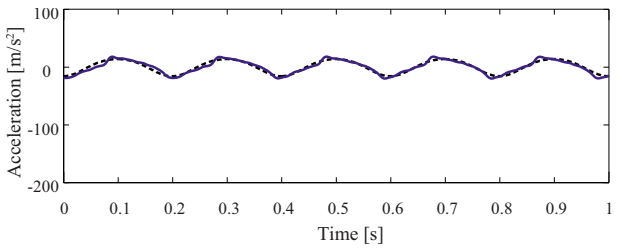

Fig. 5 Actual acceleration value of the apparatus for the control experiment (solid line) versus the calculated value (dotted line)

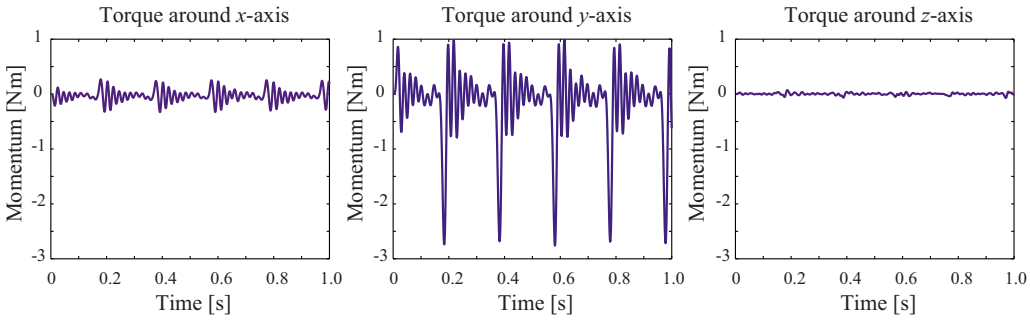

Fig. 6 Actual torque of the dual-layer prototype around *x*, *y*, and *z* axes over time when driven at 5 counts/s. The data were filtered with a seventh-order Butterworth low-pass filter (LPF) (50 Hz cutoff and 1 kHz sampling). The weight is 20 g. A mirror-symmetry pair of mechanisms counteracted the effect of the motion of linkages, i.e., torque along the *z*-axis. Torque along the *y*-axis is generated by moving the weight back and forth on the *x*-axis. The offset of the two layers produces torque in the *x*-axis, but it is smaller than that in the earlier prototype.

$$\ddot{x} = \ddot{\mu}(r - d\cos\omega t) + 2r\dot{\mu}\omega\sin\omega t + r(\mu - 1)\omega^2\cos\omega t - \frac{A - 2r^2B}{4\sqrt{l_2^2 - \{r(\mu - 1)\sin\omega t\}^2}} \quad (3)$$

where

$$A = \frac{r^4(\mu - 1)^2\{(\mu - 1)\omega\sin 2\omega t + \dot{\mu}(1 - \cos 2\omega t)\}^2}{l_2^2 - \{r(\mu - 1)\sin\omega t\}^2} \quad (4)$$

$$B = 4(\mu - 1)\dot{\mu}\omega\sin 2\omega t + \{2(\mu - 1)^2\omega^2 - (\dot{\mu})^2 - (\mu - 1)\ddot{\mu}\}\cos 2\omega t + (\dot{\mu})^2 + (\mu - 1)\ddot{\mu} \quad (5)$$

$$\dot{\mu} = \frac{-2rdl_1\omega\sin\omega t}{r^2 + d^2 - 2rd\cos\omega t} \quad (6)$$

$$\ddot{\mu} = \frac{2rdl_1\omega^2\{2rd - (r^2 + d^2)\cos\omega t\}}{(r^2 + d^2 - 2rd\cos\omega t)^2} \quad (7)$$

The motion of the weight in the slider-crank mechanism is given by

$$x = r\cos\omega t + \sqrt{l^2 - (r\sin\omega t)^2} \quad (8)$$

where $x = OD$, $r = OB$, $l = BD$, and $\omega t = DOB$ in Fig. 8. In the prototype, $r = 15$ mm and $l = 130$ mm. Acceleration of control stimuli is given by the second derivative with respect to time of x after using the Taylor series expansions as

$$\ddot{x} = -r\omega^2(\cos\omega t + \lambda\cos 2\omega t) \quad (9)$$

where $\lambda = r/l$ and λ exceeding the third order is ignored since $\lambda < 1/8$. This acceleration profile is almost a sinusoid curve. Figure 5 shows that the measured acceleration profile is more precipitous than the theoretical one. However, the symmetric property is achieved.

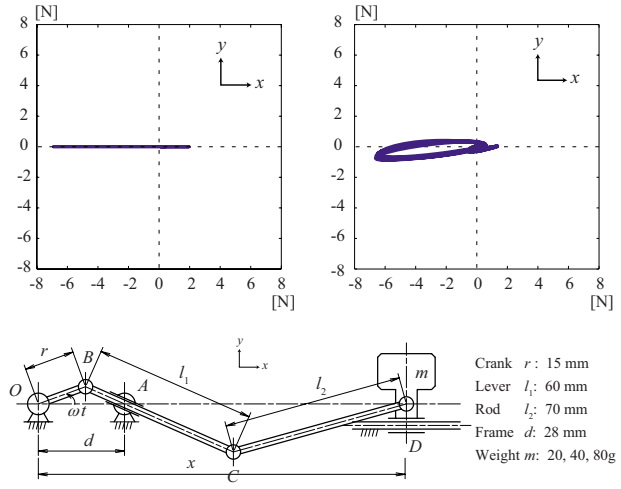

Fig. 7 Simulation of the change in the resultant force vector in the horizontal plane (upper left) and the measured value with a seventh-order Butterworth LPF (50 Hz cutoff and 1 kHz sampling) (upper right). Mechanical schematic of apparatus (lower). The weight is 20 g and the frequency is 5 counts/s. The acceleration is limited to only the *x*-axis.

3.1.3 Procedure. The aluminum box was handed to the subjects by an experimenter. The subjects were seated and were instructed to hold the box in their dominant hand and keep it as

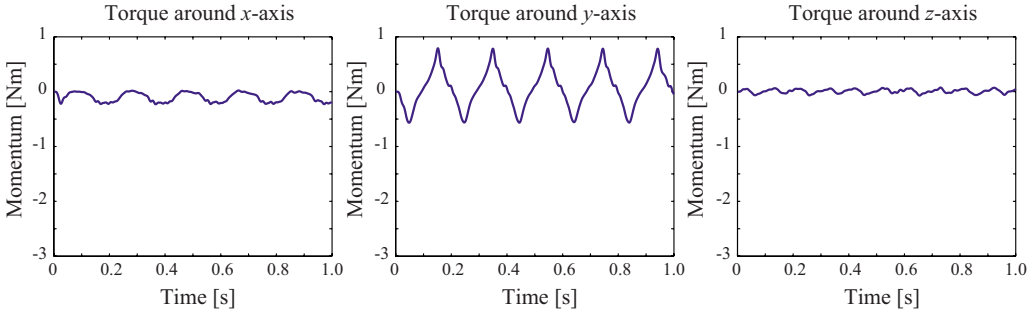

Fig. 8 Actual torque of the dual dual-layer prototype around *x*, *y*, and *z* axes over time when driven at 5 counts/s. The conditions and situation are the same as described in the caption of Fig. 6.

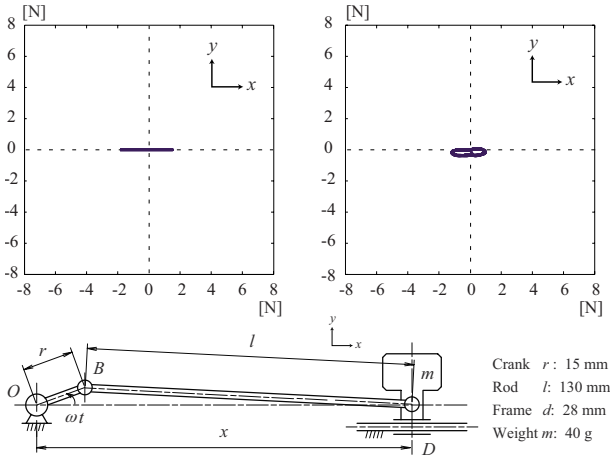

Fig. 9 Simulation of the change in the resultant force vector in the horizontal plane (upper left) and the measured value with a seventh-order Butterworth LPF (50 Hz cutoff and 1 kHz sampling) (upper right). Mechanical schematic of the apparatus (lower). The weight is 20 g and the frequency is 5 counts/s. The acceleration is limited to only the *x*-axis.

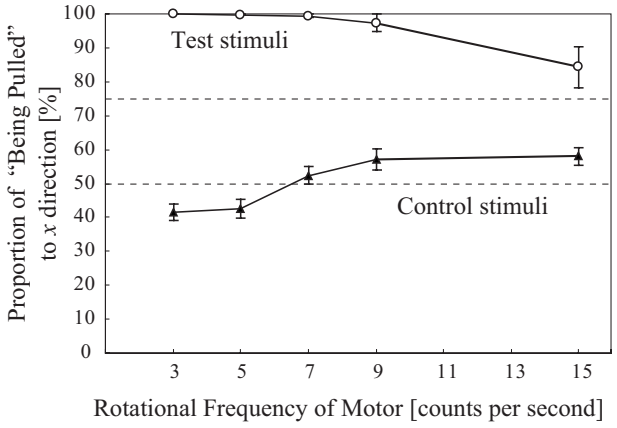

Fig. 10 Perceptual effect of acceleration profile. Average percentage-correct scores versus rotational frequencies of the motor. Each point is the percent-correct score averaged over the six subjects (100 trials per subject). The error bars show ±1S.E.

horizontal as possible. Throughout the experiment, the box was always held with the tips of the fingers wrapped around the side face of the box. To mask visual and auditory cues, subjects wore eye masks and active noise-canceling headphones throughout the experiment (Fig. 3). The noise reduction rating of the headphones is at maximum about 15 dB.

Each subject responded for five frequencies (3 counts/s, 5 counts/s, 7 counts/s, 9 counts/s, or 15 counts/s×two stimuli (test or control)×100 trials (50 forward (the direction from the crank to the slider is forward) or 50 backward (the direction from the crank to the slider is backward)), for a total of 1000 trials. The duration of each trial was about 5 s. Within each block of 50 trials, the order of presentation of the directions and frequencies was randomized. There was at least a 5 min break between each block of 50 trials to eliminate the effects of muscle strain and sensory adaptation. A binary judgment was used, in which the subjects were instructed to choose the direction of the perceived force sensation by pressing a foot pedal. The subjects were not told which frequency was used, and no feedback was given regarding the correctness of their judgments.

3.2 Results and Discussion. The experimental results for each subject are shown in Fig. 10. The horizontal axis is the rotational frequency of the motor in the device, and the vertical axis is the percent-correct score, i.e., how often the perceived force direction matched the *x*-direction (from the crank to the slider). For the test stimuli, the percentage-correct scores for all subjects at all frequencies except 15 counts/s exceeded 75%, which is the threshold. For the control stimuli, the scores were between 25% and 75%, which is the chance level. These results show that the control stimuli (symmetric acceleration) could not generate directed force sensation. We performed a binomial test for the average percent-correct scores. We found no significant effect of control stimuli for all frequencies ($p>0.05$, n.s. (not significant), one-tailed), which means that symmetric acceleration does not provide the directed force sensation. In addition, the average scores with the test stimuli (approximately 100% at frequencies under 10 counts/s) are higher than those in our previous results (at most 90% at frequencies under 10 counts/s [12]). This means the new prototype can apparently generate directed force sensation. We also performed one-way analysis of variance (ANOVA) for the percent-correct scores at the five rotation frequencies of the motor. The result was statistically significant ($F(4,20)=8.15, p<0.01$). Post hoc analyses were carried out with the Bonferroni post hoc test. The results showed that 15 counts/s were significant for the other frequencies ($p<0.05$). No significance was seen between other combinations. Therefore, frequencies lower than 10 counts/s are thought to be effective frequencies for well-perceiving force sensation. The force sensation was not effectively perceived when the frequency was over 10 counts/s.

The reasons the average scores in the current study are higher than before are thought to be the reduction in the gross weight and stable rotation of the crank by the reduction gears. Regarding the stable rotation, the amplitude of acceleration of the earlier prototype reached 43% of the theoretical acceleration peak, but that of the new one reached 85% (Fig. 11). This suggests that the substantial weight of the reciprocating mass of the earlier prototype is about half of the new one.

4 Experiment 2: Ratio of Gross Weight and Mass Weight

This experiment examined the effects of changing the gross weight and changing the weight of the reciprocating mass on the perceived force sensation. And the threshold of the ratio of the gross weight and the weight of the reciprocating mass was calculated. For this experiment, we used a binary judgment similar to that of experiment 1.

4.1 Method. Seven normal healthy adults (four women and three men) aged between 21 and 33 years participated in this experiment. Three subjects participated in experiment 1. Each subject responded for three frequencies (5 counts/s, 9 counts/s, or 15 counts/s)×three gross weights (250 g, 500 g, or 750 g) ×three reciprocating masses (20 g, 40 g, or 80 g) ×100 trials (50 forward or 50 backward), for a total of 2700 trials. A case for additional weight was attached to the aluminum box (Fig. 12). The same test stimuli as in experiment 1 were used as haptic stimuli. All other aspects of the procedure of experiment 2 were the same as in experiment 1.

4.2 Results and Discussion. Figure 13 shows the average percent-correct scores when the gross weights, the weights of the reciprocating mass, and the rotational frequencies of the motor were varied. In each graph, the horizontal axis is the rotational frequency of the motor in the device, and the vertical axis is the percent-correct score, i.e., how often the perceived force direction matched the *x*-direction (from the crank to the slider).

The results show that lighter gross weights and the heavier reciprocating mass yielded higher percent-correct scores for all frequencies (5 counts/s, 9 counts/s, or 15 counts/s). The ratio of

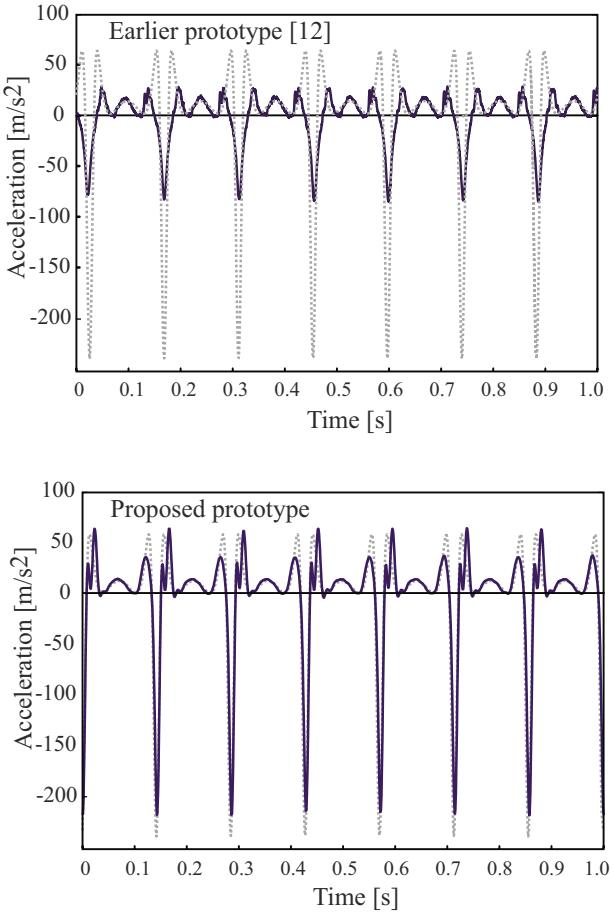

Fig. 11 Measured acceleration of earlier prototype and proposed prototype. The actual acceleration of the apparatus in the experiment is the blue solid line. The calculated one is the black dotted line. The amplitude of acceleration of the earlier prototype reached 43% of the theoretical acceleration peak, but that of the proposed one reached 85%.

the reciprocating mass and gross weight (γ) was calculated by $\gamma = m/M$, where M is the gross weight and m is the weight of the reciprocating mass. When γ increases, the average percent-correct scores in all frequencies get close to 100% (Fig. 14). On the other hand, the average percent-correct score at 5 counts/s and 9 counts/s was over 87.5% for any γ. The average percent-correct score at 15 counts/s exceeds 87.5% when $\gamma > 0.16$. We performed a two-way repeated measures ANOVA for the percent-correct scores at the three rotation frequencies of the motor and nine combinations of m and M (seven kinds of the ratio γ because two of the combinations are identical, but we treat them separately). The main effect of the rotation frequencies ($F(2,12)=6.75$, $p<0.05$; $\eta_p^2=0.53$) and the ratio γ ($F(8,48)=10.2$, $p<0.01$; $\eta_p^2=0.63$) and interactions ($F(16,96)=1.93$, $p<0.05$; $\eta_p^2=0.24$) were statistically significant. Post hoc comparisons were made using Fisher's protected least significant difference (PLSD) test. The frequencies of 5 counts/s and 9 counts/s are significantly better than 15 counts/s ($p<0.01$), and $\gamma=0.16$ or 0.32 is significantly better than the others ($p<0.05$) in the prototype. This indicates that 5 counts/s and 9 counts/s are the most effective frequencies for perceiving the force sensation in the prototype and that the ratio of the reciprocating mass to the gross weight is the dominant parameter for force perception.

The results also indicate that the frequency is more dominant for force perception than the acceleration amplitude. The acceleration amplitude is proportional to ω^2 in the prototype. The acceleration amplitude of 9 counts/s is 3.24 times of that of 5 counts/s. The average percent-correct scores for 5 counts/s at a certain m is higher than those of 9 counts/s at half of that m (e.g., the scores are higher for $M=750$ g, $m=40$ g, and $f=5$ counts/s than for $M=750$ g, $m=20$ g, and $f=9$ counts/s), even though the acceleration amplitude is smaller for the higher m. This indicates that the 5 counts/s is the dominant frequency for effective force perception.

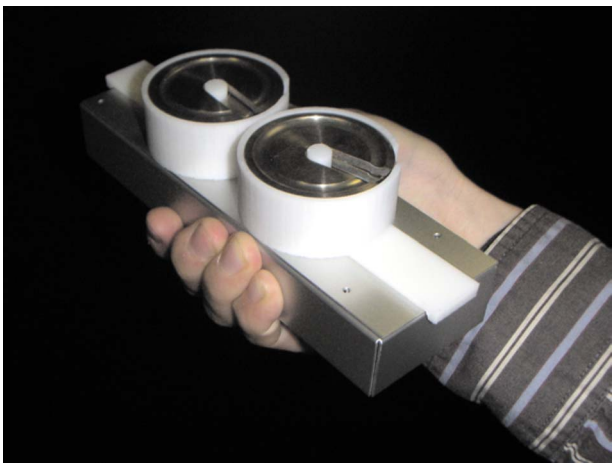

Fig. 12 Photo of the box of experiment 2. A case made of ABS was attached for additional weight.

5 Experiment 3: Holding With Nondominant Hand

The results of the above experiments showed that the holder can feel a pulling sensation with test stimuli when the device is held with the dominant hand. Here, we investigated whether the pulling sensation can be induced effectively with test stimuli when the device is held with the nondominant hand. We used binary judgment similar to that in experiment 1.

5.1 Method. Four subjects (three women and one man) from experiment 1 participated. The apparatus and the procedure were identical to those in experiment 1 except the subject held the box with the nondominant hand. Each subject responded for five frequencies (3 counts/s, 5 counts/s, 7 counts/s, 9 counts/s, or 15 counts/s)×100 trials (50 forward or 50 backward), for a total of 500 trials. The same test stimuli as in experiment 1 were used as haptic stimuli. All other aspects of the procedure of the experiment 3 were the same as in experiment 1.

5.2 Results and Discussion. The experimental results for each subject are shown in Fig. 15. For all subjects, the percent-correct scores for all frequencies exceed 85%. We performed one-way repeated measures ANOVA for the percent-correct scores at the five rotation frequencies of the motor. The result was not statistically significant ($F(4,12)=1.43$, $p=0.28$, n.s.).

Compared with the results of experiment 1, the graph shows a similar tendency for frequencies below 10 counts/s. We performed two-way repeated measures ANOVA on the percent-correct scores with the hand dominance and the five rotation frequencies of the motor by comparing the results between experiments 1 and 3 among the four subjects who participated in both. The main effect for the hand dominance was also not significant ($F(1,24)=0.96$, $p=0.36$, n.s.). An interaction effect between the hand dominance and the rotation frequencies was also not significant ($F(4,24)=1.47$, $p=0.24$, n.s.). Therefore, the results show that hand dominance does not matter for kinesthetic perception.

This indicates that there was no significant difference in perception with the dominant and nondominant hands. It also indicates that the conveyance of an effective force sensation is independent of hand dominance. At 15 counts/s, the results of experiment 3

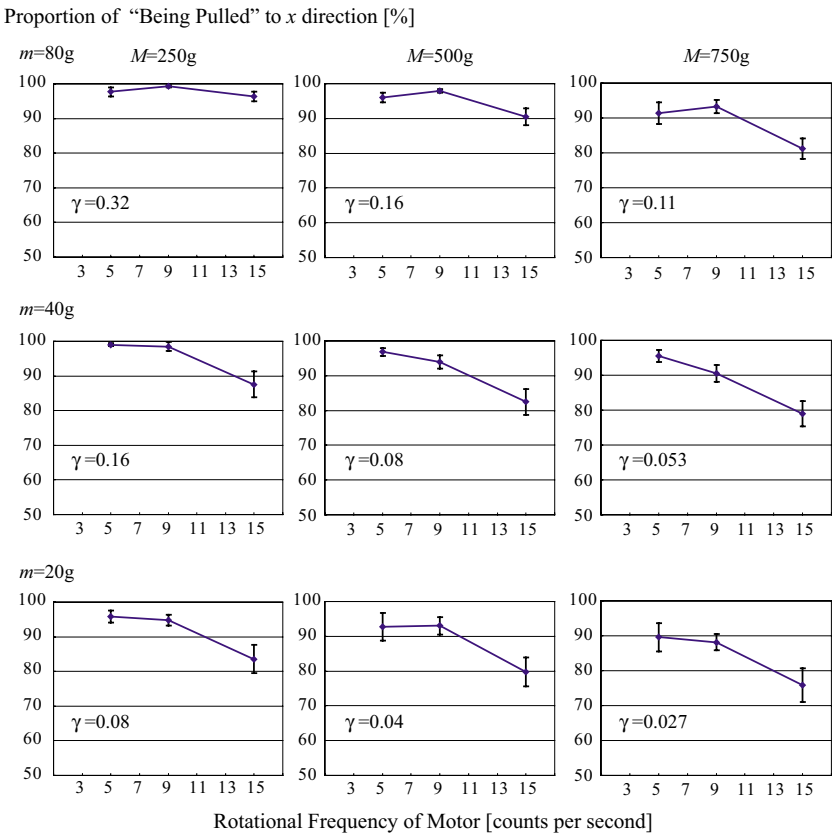

Fig. 13 Perceptual effect of gross weight of the device (columns) and the weight of the reciprocating mass in the device (rows). In columns (rows) of the graphs, the gross weight of the device (the weight of the reciprocating mass) is identical. Each point is the percent-correct score averaged over the three subjects (100 trials per subject). The error bars show ±1S.E. The *m* and *M* represent the weight of the reciprocating mass and the gross weight of the device.

show slightly higher performance than those of experiment 1, but there is no significant difference ($t(3)=1.56$, $p>0.10$).

6 General Discussion

A new prototype of a handheld force display based on a double-layer slider-crank mechanism was designed and developed. The force display conveys a sense of pulling or pushing with no external ground by taking advantage of the characteristics of human perception. Our results show that the new prototype can generate force sensation more effectively than the earlier one. This is be-

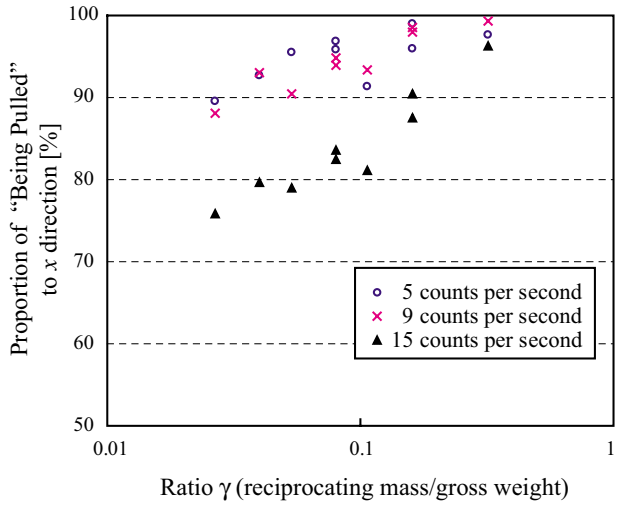

Fig. 14 Perceptual effect of the ratio of the weight of the reciprocating mass and the gross weight of the device

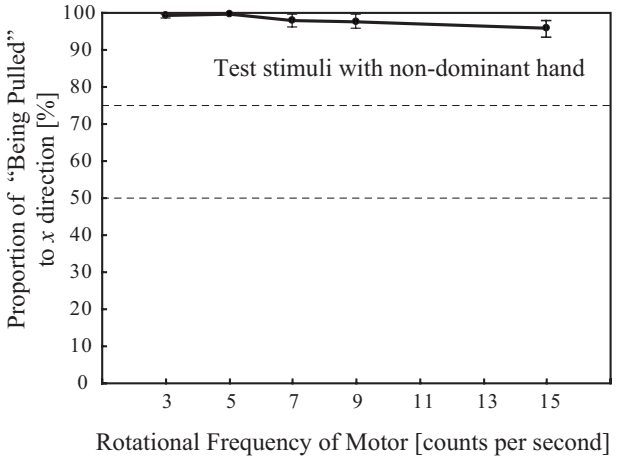

Fig. 15 Percentage-correct scores versus rotational frequencies of the motor for the dual-layer prototype when held by a nondominant hand. Average percentage-correct scores versus rotational frequencies of the motor. Each point is the percent-correct score averaged over the four subjects (100 trials per subject). The error bars show ±1S.E.

cause the gross weight of the new device becomes lower and the actual output of the acceleration amplitude becomes larger due to the stabler rotation of the crank. We demonstrated that increasing the gross weight of the device or decreasing the weight of the reciprocating mass results in worse perception of the directed force sensation.

Because the oscillation frequencies were rather low, the subjects felt the oscillation frequency. In fact, those who experienced the stimuli reported that the kinesthetic illusion generated by the asymmetric oscillation felt like an attraction force superimposed to relatively slow vibration. In addition, some of them pointed out that the force sensation induced by the stimuli was not felt smoothly compared with physical force. Future work includes examining whether the force sensation can be made as smooth as a natural continuous force sensation by changing the interpulse intervals.

From the results of experiment 1, the frequency must be in rates lower than 10 counts/s. For the design of miniature force displays, this limitation is important. This is because a miniature force display would move the reciprocating mass over a smaller stroke, leading to a decrease in the peak acceleration value. To generate a large enough force vector, a large mass would have to be used since the frequencies are fixed. However, the total gross mass of miniature force displays should be low. Although this may seem paradoxical, one of the solutions would be to use a relatively heavy object in the force display as a mass, such as a battery. Since the battery would have enough mass, if it were used as the reciprocating mass, the force generated would be large enough for mobile device application.

The reasons the gross weight plays a role in force perception may be as follows. Considering the Weber fraction of force perception, the differential threshold of force perception is thought to increase as the gross weight increases. In addition, the increase in the gross weight might work as a mass damper, which would decrease the gain of the effective pulse acceleration.

The results indicate that the percent-correct scores increase as the gross weight of the device and reciprocating weight ratio ($\gamma = m/M$) increase, and no differences were seen when $\gamma > 16\%$ in our prototype. In contrast, they show that the frequency plays an important role in the force sensation perception. This is especially true at 5 counts/s, where the subjects strongly perceived the sensation independent of γ in our new prototype. These findings can serve as criteria for designing smaller devices after comparing alternate designs. Future work includes verifying the parameters by employing another mechanism to generate the asymmetric oscillation, such as a spring-cam mechanism, in order to generalize the design criteria.

Finally, there was no significant difference in the discrimination of force direction when the device was held in the nondominant hand. This suggests the possibility that there is no dominant-hand-bias on force perception.

References

[1] Ullmer, B., and Ishii, H., 2000, "Emerging Frameworks for Tangible User Interfaces," IBM Syst. J., **39**(3–4), pp. 915–931.

[2] Luk, J., Pasquero, J., Little, S., MacLean, K., Levesque, V., and Hayward, V., 2006, "A Role for Haptics in Mobile Interaction: Initial Design Using a Handheld Tactile Display Prototype," *Proceedings of CHI 2006*, ACM, New York, pp. 171–180.

[3] Kim, Y., Britto, R., and Kesavadas, T., 2005, "Diagnostics of Arterial Pressure Pulse Using Haptic Kymograph: Remote Diagnosis of Vital Signs Through a Telehaptic Device," *Proceedings of World Haptics Conference 2005*, pp. 539–540.

[4] MacLean, K. E., Shaver, M. J., and Pai, D. K., 2002, "Handheld Haptics: A USB Media Controller With Force Sensing," *Proceedings of the IEEE VR2002 Tenth Symposium on Haptic Interfaces for Virtual Environment and Teleoperator Systems (HAPTICS 2002)*, pp. 311–318.

[5] Burdea, G. C., 1996, *Force & Touch Feedback for Virtual Reality*, Wiley, New York.

[6] Richard, C., and Cutkosky, M., 1997, "Contact Force Perception With an Ungrounded Haptic Interface," *Proceedings of the ASME Dynamic Systems and Control Division*, pp. 181–187.

[7] Yano, H., Yoshie, M., and Iwata, H., 2003, "Development of a Non-Grounded Haptic Interface Using the Gyro Effect," *Proceedings of HAPTICS 2003*, IEEE, New York, pp. 32–39.

[8] Tanaka, Y., Masataka, S., Yuka, K., Fukui, Y., Yamashita, J., and Nakamura, N., 2001, "Mobile Torque Display and Haptic Characteristics of Human Palm," *Proceedings of ICAT 2001*, pp. 115–120.

[9] Kunzler, U., and Runde, C., 2005, "Kinesthetic Haptics Integration Into Large-Scale Virtual Environments," *Proceedings of World Haptics Conference 2005*, pp. 551–556.

[10] Nakamura, N., and Fukui, Y., 2005, "Mobile Torque Display and Haptic Characteristics of Human Palm," *Proceedings of World Haptics Conference 2005*, IEEE, New York, pp. 115–120.

[11] Swindells, C., Unden, A., Sang, T., and Torque, B. A. R., 2003, "An Ungrounded Haptic Feedback Device," *Proceedings of the Fifth International Conference on Multimodal Interfaces*, pp. 52–59.

[12] Amemiya, T., Ando, H., and Maeda, T., 2008, "Lead-Me Interface for a Pulling Sensation From Hand-Held Devices," ACM Trans. on Applied Perception, **5**(3), pp. 1–17.

[13] Amemiya, T., Ando, H., and Maeda, T., 2006, "Directed Force Perception When Holding a Nongrounding Force Display in the Air," *Proceedings of Eurohaptics*, pp. 317–324.

[14] Amemiya, T., Ando, H., and Maeda, T., 2007, "Hand-Held Force Display With Spring-Cam Mechanism for Generating Asymmetric Acceleration," *Proceedings of World Haptics Conference 2007*, IEEE, New York, pp. 572–573.